Quantum stabilization of Z-strings in the electroweak model

O Schröder

School of Mathematics and Statistics, University of Plymouth, Plymouth PL4 8AA, UK

E-mail: oliver.schroder@plymouth.ac.uk

Abstract
We study the quantum energy of the Z-string in 2+1 dimensions using the phase shift formalism. Our main interest is the question of stability of a Z-string carrying a finite fermion number.

PACS numbers: 03.65.Sq, 03.70+k, 05.45.Yv, 11.27.+d

1. Introduction and motivation

Z-strings were first discovered as solutions of the classical field equations of the electroweak model by Nambu [1] in the context of bound pairs of magnetic monopoles. Later on they were rediscovered—as independent objects in their own right—by Vachaspati [2].

The main point under investigation in our study of Z-strings is their stability. If they are stable, they would be relevant for a variety of reasons: first of all, they would be the first solitonic objects in the Standard Model to be found; given the importance and ubiquitousness of solitonic objects in effective field theories in general it is surprising that they seem to play no role in the Standard Model. A second observation that might make them relevant is an alternative scenario of (electroweak) baryogenesis proposed by Brandenberger *et al* [3]. The presence of networks made from Z-strings would make the requirement (for baryogenesis to happen at the electroweak transition) of a first-order electroweak phase transition obsolete. This is an attractive scenario since the electroweak transition is known not to be of first order. A third reason for studying their stability is that—since Z-strings end in magnetic monopoles—they might contribute to the primordial magnetic field. For a general overview of applications and properties of Z-strings along with a large collection of references, cf [4].

The structure of this paper is as follows: in section 2, we briefly discuss the notion of stability in the presence of a conserved quantum number. Then, in section 3, we discuss the model under consideration, our method for computing the fermion determinant and some thoughts necessary to choose parameters properly in the ($D = 2+1$)-dimensional theory. In section 4, we present the gauge and Higgs field ansätze used for computing the fermion

determinant. Then, in section 5, we present the (preliminary) results available at the time of the *QFEXT'05* conference. In section 6, we present an outlook and some (preliminary) conclusions.

2. Stability

The question of stability is of prime importance in gauging the importance of Z-strings. At this point one should keep in mind that the Standard Model does not provide a topological stabilization mechanism for string-like objects, unlike e.g. the Abelian Higgs model. Hence every extended object has to be stable on energetic grounds. In the purely bosonic, classical sector of the electroweak model, Z-strings are solutions of the classical equations of motion. But these solutions represent only a saddle point of the classical energy functional and not a minimum. Hence, the Z-strings can decay, e.g. by condensation of ϕ_+ or W bosons along the string—so long as the value of the weak angle is close enough to its physical value; in the unphysical region $\sin \Theta_w > 0.9$ the Z-string actually is—classically—stable. These issues are discussed in depth and detail in the excellent review [4]. If one considers fermions in addition to the bosonic sector of the electroweak model, one finds that the Z-string actually binds fermions to its core, some of them rather tightly [4]. Hence, one can investigate a new kind of stability [5]: one can compare the total energy of the Z-string plus N bound fermions to the energy of N free fermions. If it is less, one has certainly found an interesting object, since even if the configuration under investigation decays further, it cannot simply decay to the vacuum (as it might in the absence of occupied bound states) since the fermion number is conserved and it has already been established that a configuration exists with energy below N times the free fermion number. However, if one wants to consider the bound-state energy of fermions one also has to take into account the fermion determinant, since it arises at the same order of an $\hbar$ (loop) expansion as the fermion bound-state energy. Thus the quantity which we consider in this paper is the difference $\Delta E(N)$ between the Z-string energy including the energy of N bound fermions and the energy of N free fermions:

$$\Delta E(N) = E_{\text{class}}(\text{Z-string}) + E_{\text{vac}}(\text{Z-string}) + \sum_{j=1}^{N} \left(\left| \omega_j^{\text{b.s.}} \right| - m \right). \tag{1}$$

Here E_{class} denotes the classical (bosonic) energy, E_{vac} denotes the renormalized vacuum polarization energy originating from the fermion determinant including effects of the counterterms and $\omega_j^{\text{b.s.}}$ denote the bound-state energies. The sum runs over the occupied levels only. The fermion number of the Z-string is N.

3. Technical prerequisites

The model we consider for our computations differs in some respects from the full electroweak model. *First* of all, we consider our fermionic weak iso-doublets to be degenerated in mass. This is the most serious of our simplifications and cannot easily be gotten rid of, since without the isospin symmetry the problem does not have enough symmetry to allow a partial wave decomposition which is at the heart of our approach to computing the fermion determinant[1]. As a *second* simplification, we drop the hypercharge field from our consideration and only consider the $SU(2)$ gauge field. This seems to be an innocuous simplification and we have techniques to deal with the $U(1)$ field. A *third* simplification that is used only to simplify the

---

[1] This channel decomposition also applies to the bound state part of the spectrum. In each channel we have a finite number of bound states which can be determined using e.g. a shooting method.

algebra is the restriction of our fermionic sector to one weak iso-doublet. The *fourth* and final simplification is that we consider the model in $D = 2+1$ dimensions[2]. Obviously, calculations in $D = 2+1$ are much simpler than in $D = 3+1$ due to the simplified UV divergence structure. And since this is only an exploratory investigation—to see whether it is worthwhile to do the vastly more complicated calculation in $D = 3+1$—it seems sensible to keep things simple where possible. But if there was no connection between results in $D = 2+1$ and $D = 3+1$, this investigation could not fulfil its purpose. Fortunately there is some evidence that the behaviour of energies and energy densities of string-like objects in $D = 2+1$ can be a good guide to the behaviour of energies (per unit length) and energy densities in $D = 3+1$. In our investigation of electromagnetic flux tubes [6, 7], we have learned that—given that the same renormalization conditions are used in $D = 2+1$ and $D = 3+1$—the renormalized quantum energies are indeed very similar in their functional dependence on widths and fluxes. We use as a working hypothesis that the same is true in the electroweak model.

The techniques used for expressing the vacuum polarization energy (which is related to the fermion determinant by dividing out the time interval T for which the determinant is evaluated) in terms of phase shifts from an associated scattering problem have been described extensively in [8] and shall be outlined here only briefly. The vacuum polarization energy can be renormalized effectively by realizing that if one replaces the full phase shifts by their Born approximation (of nth order) one gets the same result as by restricting the full one-loop vacuum polarization energy to the sum of Feynman diagrams with n external insertions of the background fields. Hence, in $D = 2+1$, the vacuum polarization energy is given by

$$E_{\text{vac}} = -\frac{1}{2} \sum_{\text{b.s.}} \left(\left| \omega_j^{\text{b.s.}} \right| - m \right) - \frac{1}{2} \int \, \mathrm{d}k \left(\sqrt{k^2 + m^2} - m \right) \sum_M \frac{1}{\pi} \frac{\mathrm{d}}{\mathrm{d}k} \left[\delta_M - \sum_{n=1}^{N} \delta_M^{(n)} \right]$$
$$+ \sum_{n=1}^{N} E_{\text{FD}}^{(n)} + E_{\text{CT}}, \tag{2}$$

where $\omega_j^{\text{b.s.}}$ denotes the fermion bound-state energies[3], δ_M the (full) phase shift in angular momentum channel M, $\delta_M^{(n)}$ its nth Born approximation; $E_{\text{FD}}^{(n)}$ is the energy contribution computed from Feynman diagrams with n external legs and E_{CT} is the energy resulting from the counterterms[4]. Note that both the k integral on the one hand and the sum of Feynman diagrams plus counterterms on the other hand are separately finite. This in particular distinguishes our investigation from the first computation of the fermion determinant in the background of a Z-string performed by Groves *et al* [10] where determinant and counterterms were individually divergent functions of the (proper-time) cut-off parameter and a finite result was only obtained by combining these two quantities. Alas, they are known only numerically, hence this procedure is numerically not stable. The other difference is that we focus on occupying bound states, whereas Groves *et al* were mainly concerned with computing the fermion determinant.

A last topic that merits discussion here is the question of how to choose the parameters of our model. In 3+1 dimensions, the gauge, Yukawa, Higgs self-coupling and vacuum expectation value of the Higgs field can be straightforwardly expressed using the fermion mass, the Higgs mass, the tree-level mass of the W boson (the W boson mass at one-loop level is a prediction based on the tree-level mass because of our choice of renormalization conditions)

---

[2] Nonetheless we use Dirac four-spinors to describe the fermions in our theory.

[3] The bound-state energies are determined from the first-order form of the Dirac equation.

[4] The calculation of the vacuum polarization energy per unit length in $D = 3+1$ uses the same phase shifts, Born approximations and bound-state energies but different kinematical factors [9]. Of course, also Feynman diagram and counterterm contributions are different.

and the Fermi coupling G_F. In 2+1 dimensions, the masses can be unambiguously re-used; however, it is not entirely obvious how to choose the Fermi coupling. It is ultimately related to a cross section—a concept that would need some translation into two spatial dimensions.

The aim of our (2+1)-dimensional calculation is to be a guide to a full (3+1)-dimensional calculation. For the vacuum polarization energy, we have assured this by using the same renormalization conditions as we would use in a $D = 3+1$ calculation.

We now fix the parameters in such a way that this is also true for the classical energy: in $D = 2+1$ we compute an energy E_{class}^{2+1}, but in $D = 3+1$ we compute an energy per unit length, E_{class}^{3+1}/L. Hence, we require

$$E_{\text{class}}^{2+1} = \frac{E_{\text{class}}^{3+1}}{L} \times \text{fundamental length},\tag{3}$$

where the fundamental length is given by half the Compton wavelength of the fermion we integrate out. This makes sense from a physical perspective, since the fermion integrated out sets the scale beyond which spatial structures can no longer be resolved. Hence a volume of thickness half the Compton wavelength of this fermion is 'perceived' as a surface. Also in the QED flux tube computations a relative factor of π/m appeared between the ($D = 2+1$)-dimensional energies and ($D = 3+1$)-dimensional energies per unit length. This prescription now allows us to express the model parameters in terms of the physical parameters of the theory in $D = 3+1$. The question on how to choose an appropriate G_F in $D = 2+1$ can thus be avoided.

4. Z-strings

We compute the vacuum polarization energy for Higgs and gauge field configurations of a specific form[5]

$$
\begin{aligned}
\phi &= \begin{pmatrix} \phi_+ \\ \phi_0 \end{pmatrix} = v \begin{pmatrix} -\mathrm{i} f_H(\rho) \cos \xi_1 + f_P(\rho) \\ f_H(\rho) \sin \xi_1 \, \mathrm{e}^{\mathrm{i}\varphi} \end{pmatrix}, \\
g \vec{W}^3 &= \frac{\hat{\varphi}}{\rho} 2 f_G(\rho) \sin^2 \xi_1, \\
\frac{g}{\sqrt{2}} \vec{W}^+ &= \frac{\mathrm{i}\hat{\varphi}}{2\rho} \, \mathrm{e}^{-\mathrm{i}\varphi} f_G(\rho) \sin 2\xi_1.
\end{aligned}
\tag{4}
$$

Here ρ denotes the two-dimensional radius, $\rho = \sqrt{x^2 + y^2}$, and $\hat{\varphi}$ is the unit vector in the azimuthal direction. The Higgs vacuum expectation value is given by v. The gauge coupling is given by g. The functions $f_H(\rho)$, $f_P(\rho)$ and $f_G(\rho)$ are *profile functions* and are discussed in the remainder of this section. The requirement of finite classical energy necessitates for $\rho \to 0$ both $f_H \to 0$ and $f_G \to 0$. For $\rho \to \infty$, $f_G \to 1$ and $\phi^\dagger \phi = |f_H|^2 + |f_P|^2 \to 1$ are required. As ξ_1 is changed from $\frac{\pi}{2}$ to 0 the configuration is changed continuously from the Z-string to a purely scalar configuration without winding. Note that in this process the gauge invariant length $\phi^\dagger \phi$ of the Higgs field does not change since it is independent of ξ_1. The classical energy is a continuous function of ξ_1 which—for $f_P \equiv 0$—has a maximum at $\xi_1 = \pi/2$ and decreases continuously as $\xi_1 \to 0$. This illustrates our earlier statement that the Z-string is classically unstable and can unwind without hitting a topological barrier.

The ansatz shown in (4) is a subset of a more general ansatz called the *sphaleron square*, cf also [11].

---

[5] In the absence of the hypercharge field, the Z-field reduces to the W^3-field. $\vec{W}^+$ is the conventional charged W field, ϕ_0 denotes the neutral Higgs field and ϕ_+ the charged Higgs field.
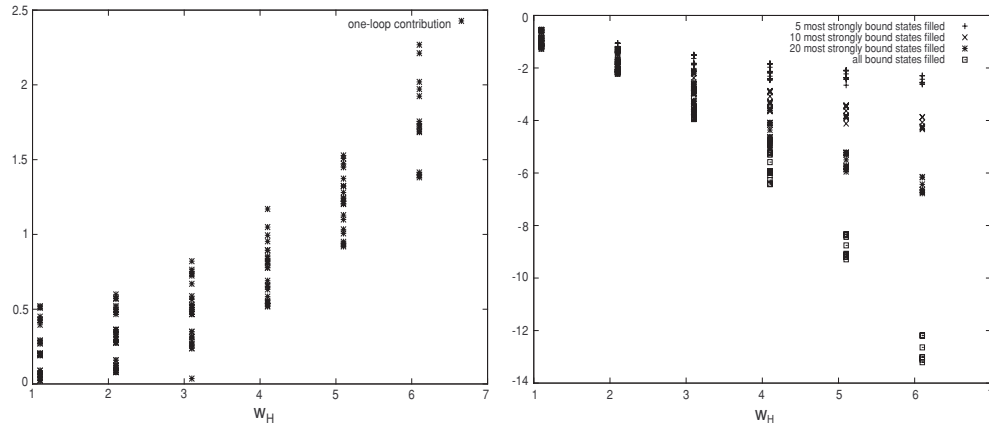
Figure 1. The left panel shows the (completely renormalized) vacuum polarization energy as a function of the width w_H, the right panel shows the energy gained by filling bound-state levels relative to the same number of free fermions, $\sum_{j=1}^{N}(|\omega_j^{\text{b.s.}}|-m)$ for $N = 5, 10, 20$ and all available bound states. Note that this latter curve corresponds to comparing configurations with different fermion number.

For our numerical investigations we cannot deal with general profile functions, but rather need also ansätze for the functions that have the proper behaviour for small and large ρ:

$$f_H(\rho) = 1 - \mathrm{e}^{-\frac{\rho}{w_H}}, \qquad f_P(\rho) = a_P\, \mathrm{e}^{-\frac{\rho}{w_P}}, \qquad f_G(\rho) = 1 - \mathrm{e}^{-\frac{\rho^2}{w_G^2}}. \tag{5}$$

Altogether we have four parameters (plus ξ_1): three widths w_H, w_G, w_P and one amplitude a_P—the amplitudes for f_H, f_G are fixed by requirements of finite classical energy mentioned above.

5. Results

In this section we present a couple of preliminary results for classical, vacuum polarization and bound-state energies. The plots in figures 1–3 have in common that we have fixed $\xi_1 = \frac{\pi}{2}$, i.e. we present results for the Z-string configuration.

Couplings and Higgs vacuum expectation value are determined by our choice of masses and the Fermi coupling. We choose for the fermion mass 170 GeV, for the Higgs mass 115 GeV, for the tree-level W boson mass 80 GeV and for the Fermi coupling 10^{-5} GeV^{-2}.

When studying the plots the following point has to be kept in mind: since ξ_1 is fixed, we have a four-parameter numerical problem. The plots are only standard two-dimensional plots; hence energies can only be plotted as a function of a single variable. We have chosen NOT to fix the other parameter values but plot the energies of all the configurations that we have available. Hence, for each observable there is not a curve but a band corresponding to the ranges of the variables not represented on the x-axis of the plot. In figure 1 we show in the left panel the renormalized vacuum polarization energy (in units of the fermion mass) including Feynman diagrams and counterterm contributions as a function of the width of the neutral Higgs field, w_H. This seems to be the predominant dependence. The contents of the right
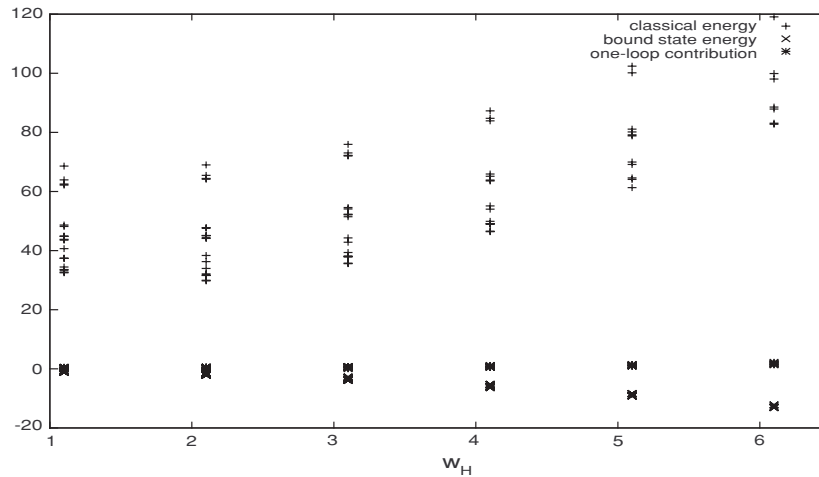
Figure 2. The figure shows the classical energies (upper band of points), vacuum polarization energies (denoted by 'one-loop contributions', medium band of points) and $\Delta E^{\text{b.s.}}$(all) (lower band of points) as a function of the width w_H.

panel are slightly more difficult to explain: in (1) only one part of $\Delta E(N)$ depends on the fermion number of the configuration, namely

$$\Delta E^{\text{b.s.}}(N) = \sum_{j=1}^{N} \left(\left| \omega_j^{\text{b.s.}} \right| - m \right). \tag{6}$$

Since we look for a stable object we restrict our choice of bound states in (6) to the most strongly bound states. In the right panel of figure 1 we now plot $\Delta E^{\text{b.s.}}(N)$ for $N = 5, 10$ and 20. For the lowest curve we occupy *all available* bound states, denoted in the following as $\Delta E^{\text{b.s.}}$(all). Thus, points along this curve can and will correspond to different fermion numbers. Whereas the curves with fixed fermion number level off as w_H increases, this latter curve keeps decreasing as w_H increases. This is due to an amazing proliferation of bound states. Whereas for $w_H \approx 2$ there is only a handful of bound states, for $w_H \approx 6$ there can be easily more than 80 bound states. The dependence of the number of bound states seems to be roughly quadratic—as w_H increases, both more and more angular momentum channels contain bound states and the number in each individual channel keeps increasing as well. More recent investigations, performed after *QFEXT'05*, show that this behaviour continues at least up to widths $w_H \approx 12$. In this parameter regime, we have found configurations with around 500 bound states in various angular momentum channels.

In figure 2, we plot the classical energy, the vacuum polarization energy and $\Delta E^{\text{b.s.}}$(all). This figure clearly shows the different orders of magnitude that are involved. Furthermore, it can be clearly seen that the effect of populating bound states by far outweighs the increase in energy due to taking into account the fermion determinant.

When combining the classical energy with the vacuum polarization energy and $\Delta E^{\text{b.s.}}(N)$ to form $\Delta E(N)$, one has to keep in mind that the fermions—in contrast to the bosons in this model—carry a colour quantum number and that fermions with different colours are energetically degenerate. Hence, both E_{vac} and $\Delta E^{\text{b.s.}}(N)$ have to be multiplied by the number of colours N_C before they are added to E_{class}. The fermion number under consideration then is actually $N \times N_C$.
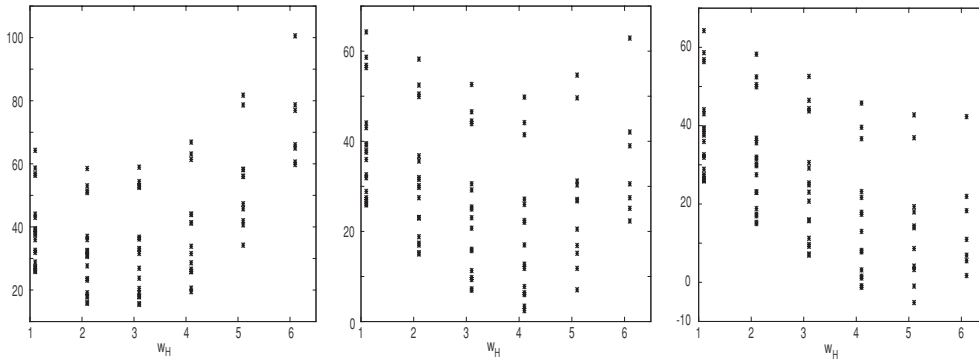
Figure 3. In this figure, we present our results for $\Delta E(N)$ as a function of the width w_H for different values of N, from left to right $N = 10, 30, 50$. The actual fermion numbers are (again from left to right) 90, 270, 450.

In figure 3, we use $N_C = 9$. In the left panel of figure 3 we have filled the ten most strongly bound states. We find a minimum, but since we plot ΔE this minimum has to be below zero to indicate a stable object. So for both $N = 10$ and $N = 30$ (panel in the middle) the object under consideration is not stable. The situation is different for $N = 50$, since the minimum there is clearly below zero. Since N does not include the colour degeneracy this stable object actually carries fermion number 450.

Also, a certain pattern seems to emerge from figure 3: as N increases, the minimum of $\Delta E(N)$ moves towards larger values of w_H and the value of $\Delta E(N)$ at the minimum decreases. This is of course due to the fact that the larger w_H the more actual bound states are available and hence the possible gain in energy by filling these bound states also increases. It may even be possible that for sufficiently large w_H, the energy gain is large enough to allow a stable object even for $N_C = 3$ to exist, but this is a question under current investigation and cannot be answered at the moment.

A different investigation—results will have to be reported elsewhere—considers a heavy fermion with masses around 1.5 TeV instead of the top quark mass used here.

6. Conclusions

For this contribution only preliminary data were available. Nevertheless we can state that— given a sufficient number of colours—we have found a very interesting object that is stable in the sense of section 2. It is very large and carries a gigantic fermion number (450). At the moment it is not clear what happens if we increase the size of the object further—will we find so many bound states that maybe it is possible to find a stable object even for $N_C = 3$? Therefore an in-depth investigation of the parameter space is urgently needed, and is already under way [12]. Also, the great effort to investigate the $D = 3+1$ case is now fully justified.

Acknowledgments

References

[1] Nambu Y 1977 String-like configurations in the Weinberg–Salam theory *Nucl. Phys.* B **130** 505
[2] Vachaspati T 1992 Vortex solutions in the Weinberg–Salam model *Phys. Rev. Lett.* **68** 1977–80
    Vachaspati T 1992 Vortex solutions in the Weinberg–Salam model *Phys. Rev. Lett.* **69** 216 (erratum)
[3] Brandenberger R H and Davis A-C 1993 Electroweak baryogenesis with electroweak strings *Phys. Lett.* B **308** 79–84
[4] Achucarro A and Vachaspati T 2000 Semilocal and electroweak strings *Phys. Rep.* **327** 347–426
[5] Khemani V 2003 Quantum solitons in the electroweak theory Talk given at *QFEXT'03* (*Preprint* hep-th/03120249)
[6] Graham N, Khemani V, Quandt M, Schroeder O and Weigel H 2005 Quantum QED flux tubes in 2+1 and 3+1 dimensions *Nucl. Phys.* B **707** 233–77
[7] Weigel H 2006 Energies of quantum QED flux tubes *J. Phys. A: Math. Gen.* **39** 6799
[8] Graham N, Jaffe R L and Weigel H 2002 Casimir effects in renormalizable quantum field theories *Int. J. Mod. Phys.* A **17** 846–69
[9] Graham N, Jaffe R L, Quandt M and Weigel H 2001 Quantum energies of interfaces *Phys. Rev. Lett.* **87** 131601
[10] Groves M and Perkins W B 2000 The dirac sea contribution to the energy of an electroweak string *Nucl. Phys.* B **573** 449–500
[11] Klinkhamer F R and Olesen P 1994 A new perspective on electroweak strings *Nucl. Phys.* B **422** 227–36
[12] Graham N, Khemani V, Quandt M, Schroeder O and Weigel H in preparation
[13] Vermaseren J A M 2000 New features of FORM *Preprint* math-ph/0010025
[14] Wolfram Research Inc. *Mathematica* (Champaign, IL)